Food Biophysics (2025) 20:127
https://doi.org/10.1007/s11483-025-10016-5

RESEARCH

3D Printing of Unconventional Starches from Andean Tubers: Microstructural, Textural, and Rheological Properties

Luis Daniel Daza[1,2] · **Cristina Reche**[1] · **Angélica Sandoval-Aldana**[2] · **Henry Alexander Váquiro**[2] · **Valeria Soledad Eim**[1]

Received: 11 March 2025 / Accepted: 6 August 2025 / Published online: 19 August 2025
© The Author(s) 2025

Abstract
This study evaluated the potential of unconventional starches extracted from Andean tubers, ulluco (Ullucus tuberosus) and cubio (Tropaeolum tuberosum), as raw materials for 3D food printing. Gels were formulated with starch concentrations of 8%, 10%, and 12% (w/v) and characterized in terms of microstructure and rheological properties. Both starches exhibited suitable printability, attributed to their pseudoplastic flow behavior. However, the hardness of the printed structures varied depending on starch type and concentration. Cubio starch showed higher hardness at both low and high concentrations (8% and 12%), whereas ulluco starch exhibited its highest hardness at the lowest concentration. Microscopic analysis revealed reticulated networks whose homogeneity was influenced by the degree of gelatinization and the starch content in the matrix. The printed gels demonstrated good resilience, variable hardness, and low crystallinity, indicating thermal-induced disruption of the native ordered structure. Rheologically, the samples showed viscoelastic behavior dominated by the elastic modulus (*G'*) and fitted the power-law model. These findings support the technological feasibility of ulluco and cubio starches as functional ingredients for the development of customized or functional foods through additive manufacturing technologies. Their application may foster the utilization of underused crops and contribute to the diversification of raw materials in the food industry.

Keywords Printability · Gelatinization · Non-conventional starches

Introduction

Three-dimensional (3D) printing is an emerging technology that produces physical structures by depositing a material or a material blend layer by layer, resulting in a product with predetermined size and shape characteristics [1, 2]. This technology offers various production advantages for the food industry, including product customization in shape, size, sensory and nutritional properties; optimization and automation; waste reduction; and cost-effectiveness improvement [3, 4]. For instance, Kim et al. [5]. designed a low-calorie formulation to produce surimi by 3D printing with a protein analog, obtaining texture and salinity characteristics similar to those of commercial surimi. Similarly, Bebek et al. [6]. produced 3D printed snacks from strawberry products with antioxidant and antimicrobial potential, meeting nutritional needs and ensuring stability of the printed food during storage.

However, 3D food printing requires, during the design process of food inks, the incorporation of raw materials that meet specific nutritional requirements such as proteins, vitamins, and others, as well as additional components that not only provide nutritional value but also contribute to the structural properties of the product. This is essential to ensure the physical integrity of the printed food and to prevent its collapse during production, transportation, and storage [7]. Consequently, the materials used for this purpose (structural integrity) must have malleability, self-support, rapid solidification, and a specific level of fluidity that can generate a smooth extrusion from the printer's extrusion

✉ Luis Daniel Daza
lddazar@ut.edu.co

[1] Department of Chemistry, University of the Balearic Islands, Ctra Valldemossa, km 7.5, Palma de Mallorca, Baleares 07122, Spain

[2] Departamento de Producción y Sanidad Vegetal, Facultad Ingeniería Agronómica, Universidad del Tolima, Ibagué 730006, Colombia

head. Additionally, the materials must form a stable and resistant structure on the printing platform [1]. Due to the limited availability of materials suitable for 3D printing of food, there is a need for alternative options that can meet the requirements of food design and enable the total industrial leverage of this technology [3].

Starch contributes 50–70% of the energy intake in the human diet and is abundantly found in a wide range of plant-based foods [8]. Several authors have reported that starches from different botanical sources exhibit the typical shear-thinning behavior of pseudoplastic fluid. This attribute is closely related to the ease of extrusion, which makes starch an attractive raw material for 3D printing [9, 10]. Moreover, the retrogradation process that occurs after heating and gelatinizing the starch leads to the leaching of amylose and amylopectin and their subsequent reorganization, resulting in improved hardness and shape retention of the 3D print [10, 11]. The printability of starch is influenced by different factors such as amylose content, granule size, amylose: amylopectin ratio, pasting properties, and starch concentration, among others, which vary depending on the botanical source.

Although different types of starch have been tested for 3D printing of food products and their effects on rheological [12, 13], textural and printability properties [14, 15] have been assessed, most studies have focused on commercial starches. However, the continuous growth of the global population and the resulting increase in starch demand from both food and non-food industries can hardly be met without compromising food security. This, in turn, may contradict the principles of the Sustainable Development Goals (SDGs), particularly those related to zero hunger, responsible consumption and production, and the sustainable management of natural resources. Therefore, the search for new or non-conventional sources of starch emerges as a potential alternative to address this challenge. Nonetheless, these sources must provide, on the one hand, high extraction yields and suitable techno-functional properties for industrial applications, and on the other hand, contribute to mitigating food insecurity while adding value to underutilized or traditional crops from specific regions. In this context, Andean tubers represent a promising source of non-conventional starches with potential applications in the agri-food industry. Among them, *Tropaeolum tuberosum* (commonly known as cubio) and *Ullucus tuberosus* (ulluco) stand out as underutilized raw materials, with starch contents exceeding 40% and 65% on a dry basis (d.b.), respectively [16, 17].

Cubio, also referred to as "mashua," "añu," or "isaño," is an Andean tuber belonging to the family Tropaeolaceae and the genus *Tropaeolum*. It is cultivated from Colombia to northern Argentina at altitudes ranging between 2000 and 4300 m a.s.l [18]. The starch extracted from cubio exhibits amylose contents between 26% and 31% (d.b.) [17, 19, 20], and small granule sizes (5.36–62.34 µm). Furthermore, it demonstrates good thermal stability during gelatinization, and a considerable increase in the final viscosity of the gel [17, 19–21]. Ulluco, in turn, belongs to the family Basellaceae and is cultivated at similar altitudes (2400–4250 m.a.s.l.) as cubio [22]. Its starch contains amylose levels ranging from 28 to 35% (d.b.) [16, 17], with particle sizes varying from 5.68 to 32.6 µm, and average values reaching up to 560.2 µm, depending on the analytical methodology employed [17, 21]. It has been previously demonstrated that ulluco and cubio starches exhibit greater stability in aqueous dispersions than commercial potato starch, especially at pH values equal to or below 7, which are typical of many food systems [21]. This enhanced stability may improve compatibility with other ingredients, enhance the rheological properties of bio-inks, and increase the structural stability of printed objects after the 3D printing process. Additionally, it has been shown that cubio and ulluco starches exhibit high thermal stability, based on the analysis of their pasting properties, in comparison with commercial potato starch. Although the latter is known for reaching a high peak viscosity, it undergoes a significant loss of stability during both the breakdown phase and the cooling stage, where leached molecules reorganize. This behavior is not observed in starches derived from Andean tubers, which maintain a more stable structure throughout the process, an attribute that represents a potential advantage for their application in 3D printing [16, 20].

Considering the SDGs, the need to add value to underutilized crops, and the growing demand for new sources of raw materials to help mitigate food insecurity in both traditional and emerging industries—such as 3D food printing—this study aims to evaluate the use of unconventional starches derived from cubio and ulluco in the preparation of 3D-printed structures at different concentrations, and to analyze their physical and rheological properties.

Materials and Methods

Raw Material

The Andean tubers were obtained from the local market. Ulluco starch (ULS; apparent amylose content of 27.9%; relative crystallinity: 17.1%; particle size 1.79 to 138 µm, protein 0.22% d.b., lipids 0.11% d.b., ash 0.12% d.b., pasting temperature 90 °C) and Cubio starch (CUS; apparent amylose content of 31%; relative crystallinity: 16%, particle size 1.37 to 53.3 µm, protein 0.16% d.b., lipids 0.25% d.b., ash 0.21% d.b., pasting temperature 60.7 °C) were obtained and characterized as previously reported [16, 23].

Sample Preparation and 3D Printing

The starch gels pastes were prepared by mixing the material at different concentrations (8%, 10%, and 12% w/v) with distilled water. The selection of concentrations was based on preliminary analyses (data not shown), which revealed that formulations with concentrations below 8% immediately lost their structural integrity, while concentrations above 12% caused clogging of the printer cartridge, preventing proper structure formation. The mixture was heated to 90 ± 2 °C with constant stirring using a mechanical stirrer (RZR 2021, Heidolph, Germany) at 180 rpm for 10 min. Once the sample reached a temperature of 60 °C, it was transferred to a print cartridge (1.5 mm nozzle) and maintained at this temperature throughout the printing process. The 3D printing was carried out in an extrusion-based 3D printer (Foodini™, Natural Machines, Spain). A cuboid model with dimensions of 20 mm × 20 mm × 10 mm was printed with a monolayer height and nozzle movement speed of 1.4 mm and 500 mm × min^{-1}. For the dynamic-mechanical analysis (DMA), specimens with dimensions of 10 mm × 10 mm × 5 mm were printed. The samples were coded according to the starch source; ulluco starch was identified as ULS and cubio starch as CUS, followed by the corresponding concentration (Thus, the 3D printing of ULS at 8% will be called ULS8).

Microstructure of 3D Prints

The microstructural characteristics of the 3D print samples were visualized using scanning electron microscopy (SEM/S-3400 N, Hitachi, Germany). Prior to analysis, the samples were lyophilized for 72 h using a freeze dryer (BK-FD12PT, Biobase Bioindustry, China) and freeze-fractured using liquid nitrogen. Then, the samples were placed on stubs using double-sided carbon tape. Images were obtained at an accelerating voltage of 15 kV and under a vacuum pressure of 40 Pa at varying degrees of magnification.

X-Ray Diffraction

The X-ray diffraction XRD was carried out using a Bruker D8 ADVANCE diffractometer (Bruker, USA) operating with Ni-filtered under the condition of Cu-Kα radiation (λ = 1.5406 Å and at 40 kV and 40 mA). The 3D-printed samples were stabilized at room temperature for 1 h, then frozen, freeze-dried, and ground using an analytical grinder universal mill (Yellowline A10, IKA, Germany). Data collection was carried out in the 2θ range of 3.5–70°, with a step size of 0.02035° (2θ) and a counting time of 0.8 s $step^{-1}$. Relative crystallinity was calculated using the DIFFRAC.EVA software (Bruker, USA).

Texture Analysis

Textural analysis was performed using a universal test machine (Zwick/Z100, Zwick Roell, Germany). The gels were analyzed by being compressed twice to 40% of the total sample height at a speed of 6 mm × min^{-1} using a cylindrical probe with an initial gap of 13 mm. The hardness, springiness, and cohesiveness were reported as the mean of at least five repetitions.

Dynamic-Mechanical Analysis

The dynamic mechanical analysis (DMA) was conducted using a dynamic mechanical analyzer (DMA, Q800, TA Instruments, USA) equipped with a parallel plate geometry (20 mm diameter and 10 mm gap). After allowing the samples (10 mm × 10 mm × 5 mm) to rest for 1 hour following printing, they were subjected to compression testing in a "frequency sweep" mode, ranging from 0.1 to 30 Hz at a fixed strain amplitude of 1 ± 0.004% of the total sample height. The test was performed at room temperature (24 ± 2°C) [24]. The resulting storage modulus (*G'*) and loss modulus (*G"*) were obtained and analyzed using Universal Analysis 2000 V3.9 A software (TA Instruments, Japan). The power law equation (Eq. 1) [25] was used to model the dependence of *G'* on frequency. Results are presented for printed pastes that demonstrated sufficient stability for measurement.

$$G' = K \bullet \omega^{n'} \quad (1)$$

where *K* is related to the viscoelastic properties of the material (power law constant) (MPa Hz^{-1}); ω is the frequency (Hz), and *n'* is the frequency exponent (dimensionless).

Statistical Analysis

The results were reported as each property's mean and standard deviation based on at least three replicates for each sample. Analysis of variance (ANOVA) and Tukey–Kramer range tests at a significance level of 0.05 were performed to compare the properties of the 3D prints.

Results and Discussion

Printability and Morphology of 3D Printed Starch

The microstructure and visual aspect of the 3D prints extruded gel pastes are shown in Fig. 1. Samples prepared using ULS and CUS presented good stability and printability. However, all ULS samples showed poorly defined

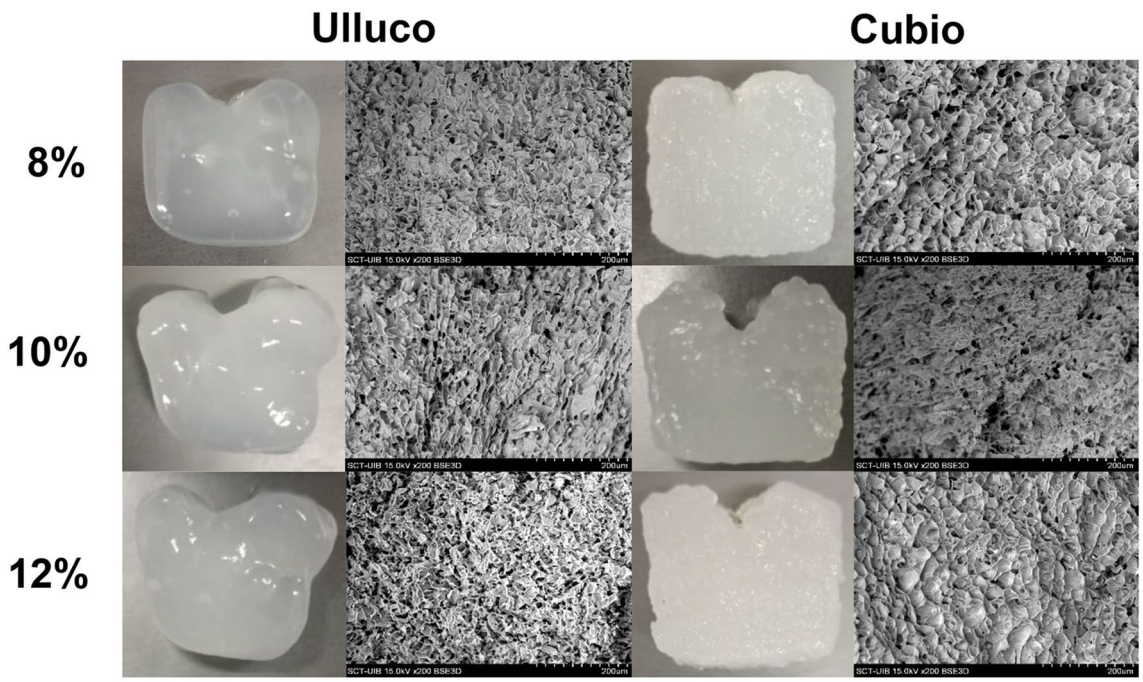


Fig. 1 3D prints and SEM micrographs of 3D prints based on ulluco and cubio starches prepared at different starch concentrations: 8%, 10%, and 12%

geometries with rounded shapes (low precision with the cubic model used). In contrast, the CUS samples had better-defined geometries, as evidenced by the presence of straight lines. However, rounded corners were also observed. Using either starch, the best geometry was obtained with the lowest material concentrations (ULS8 and CUS8). This behavior could be related to the higher viscosity of pastes with higher starch concentration, which could limit the ease of extrusion and formation of the printed figure. Similar observations were made for 3D printing of potato starch at different concentrations (0%, 1%, 2%, and 4%) combined with mashed potatoes, where it was evidenced that the sample without starch was easy to print but quickly lost structure. Moreover, the authors observed that low starch concentrations (1% and 2%) improved the printability of the gel pastes, which was related to the values of shear stress and the storage modulus of the gel paste [26].

Micrographs of the samples showed the formation of reticulated, lamellar, or modular cell-like structures. Increasing the starch concentration in the samples prepared with ULS resulted in higher cell density in the structure. These structures can be associated with complete or partial starch gelatinization and cross-linked interactions between polymer chains [27]. However, higher starch concentration also hindered gelatinization, and structures with incomplete gelatinization were observed, leading to material agglomeration. The degree of gelatinization depends on gelatinization time and process temperature and can affect the microstructure of the print. Cheng et al. [28]. demonstrated that low or high processing temperatures could affect the microstructural integrity of 3D-printed corn starch (15 min of gelatinization). The authors found that a temperature of 65 °C generated a partial gelatinization of the starch, and thus, the structure could not achieve adequate crosslinking; on the contrary, temperatures above 80 °C caused microfractures in the structure, which was associated with the presence of short chains that have less interaction capacity. Samples prepared with CUS had a similar cell structure to samples prepared with ULS but with a larger size. Except for the CUS10 sample, which presented a high cell density and porosity, the other samples prepared with CUS had a highly compact microstructure with decreased observed pores. Similar structures were observed in 3D printing using corn, wheat, and potato starches at a concentration of 25%. According to Zheng et al. [14]. more compact structures result in firmer prints with more resistance to loss of integrity. The microstructure of 3D prints can also affect other properties, such as the mechanical properties and overall integrity of the structure. However, the microstructure of 3D prints prepared with starches depends on different factors such as the processing conditions (temperature, equipment, printing cartridge) and the physicochemical properties of the starch (amylose and amylopectin content, pasting properties, size, or degree of polymerization (DP) of the chains, gelatinization temperature among others).

The appearance of pores in some of the analyzed structures is directly associated with the gelatinization process of starch granules, a phenomenon that occurs at temperatures

above 60 °C in the presence of excess water. Initially, water penetrates the amorphous regions of the granule, primarily composed of amylose, causing it to swell. As the temperature increases, water also accesses the crystalline regions, predominantly formed by amylopectin, leading to the progressive disorganization of the granule's internal structure through the disruption of hydrogen bonds and the formation of new bonds between water and the starch polysaccharide chains [29]. Subsequently, the irreversible rupture of the granule occurs, allowing the leaching of amylose into the aqueous medium, followed, under prolonged temperature and time conditions, by the partial release of amylopectin. During the cooling phase, amylose chains tend to reorganize through hydrogen bonding, forming a three-dimensional network that immobilizes water and results in the formation of a gel. The microstructure of this gel may exhibit porosity, which depends on factors such as starch concentration, cooling rate, and post-processing treatments like thermal or freeze-drying [30].

Crystallinity of 3D Printed Starch

The crystallinity patterns of the samples are shown in Fig. 2. The relative crystallinity values of samples prepared using ULS were 1.8%, 1.9%, and 2.0% for ULS8, ULS10, and ULS12, respectively. The relative crystallinity for samples obtained with CUS were 1.3%, 1.7%, and 1.9% for CUS8, CUS10, and CUS12, respectively. All samples displayed signals at 17° at a diffraction angle of 2θ. The presence of a single low-intensity signal associated with crystallinity patterns indicates the loss of the ordered structure of the native starch granule, which can be attributed to the gelatinization of starch granules during the thermal process, as well as the retrogradation of the amylose and amylopectin chains. Previous studies reported that the diffraction pattern of ULS and CUS corresponds to type-B with diffraction peaks at 5.6°, 15°, 17°, 20°, 22° and 24° 2θ [11, 31]. Liu et al. [27]. evaluated the impact of printing temperature on the crystallinity of potato starch-based 3D prints. They observed that low printing temperatures (60 °C) partially preserved the type-B diffraction pattern in the samples regardless of the starch concentration. However, at 70 °C, the signals corresponding to the crystalline regions of the samples vanished completely. Ahmadzadeh & Ubeyitogullari [32] also reported relative crystallinity (ranging from 5.64 to 8.78%) in 3D prints based on corn starch at different concentrations. This relative crystallinity is associated with the recrystallization of the amylose and amylopectin chains, and it can be related to the textural properties since a higher crystallinity implies a higher ordering of the polymer chains.

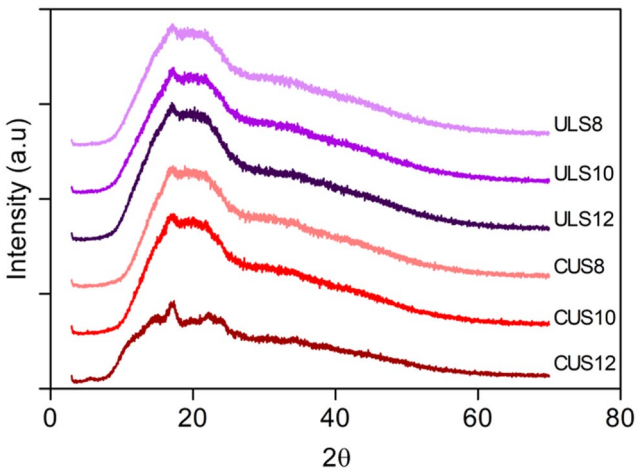


Fig. 2 XRD diffractogram of 3D prints based on ulluco and cubio starches prepared at different starch concentrations: 8%, 10%, and 12%

During the pasting and heating process of starch, the increase in temperature induces granule swelling due to water penetration, leading to the dissolution and disorganization of both amorphous and crystalline regions. Subsequently, granule rupture occurs, followed by the leaching of amylose and amylopectin into the surrounding medium [33]. As observed in previous studies, ulluco starch and mashua starch have the ability to reorganize and contribute to an increase in final viscosity [16, 20]. In 3D-printed materials, the loss of crystallinity may suggest a reduction in specimen hardness, considering that higher molecular organization is generally associated with greater resistance to deformation. Furthermore, printability is influenced by the degree of starch crystallinity, as lower crystallinity is associated with higher water retention capacity, which facilitates extrusion and improves interlayer cohesion during additive manufacturing [34]. However, other factors also affect the properties of the 3D printed materials, such as the size or degree of polymerization of amylopectin and gelatinization properties. In this work, no relationship was established between the relative crystallinity value of the samples obtained with ULS and the microstructure since a higher ordering was expected in the samples with higher starch concentration. However, the ULS10 and ULS12 samples showed partial gelatinization, so their relative crystallinity value was similar to that of ULS8, which may affect the textural properties (as observed in Sect. Textural Properties of 3D Printed Starch). Additionally, the samples prepared with CUS showed a direct relationship between the relative crystallinity and the starch concentration.

Textural Properties of 3D Printed Starch

The hardness, springiness, and cohesiveness of 3D samples based on ULS and CUS are shown in Fig. 3. Hardness is a parameter associated with shape retention and softness of the 3D material, which is important for sensory

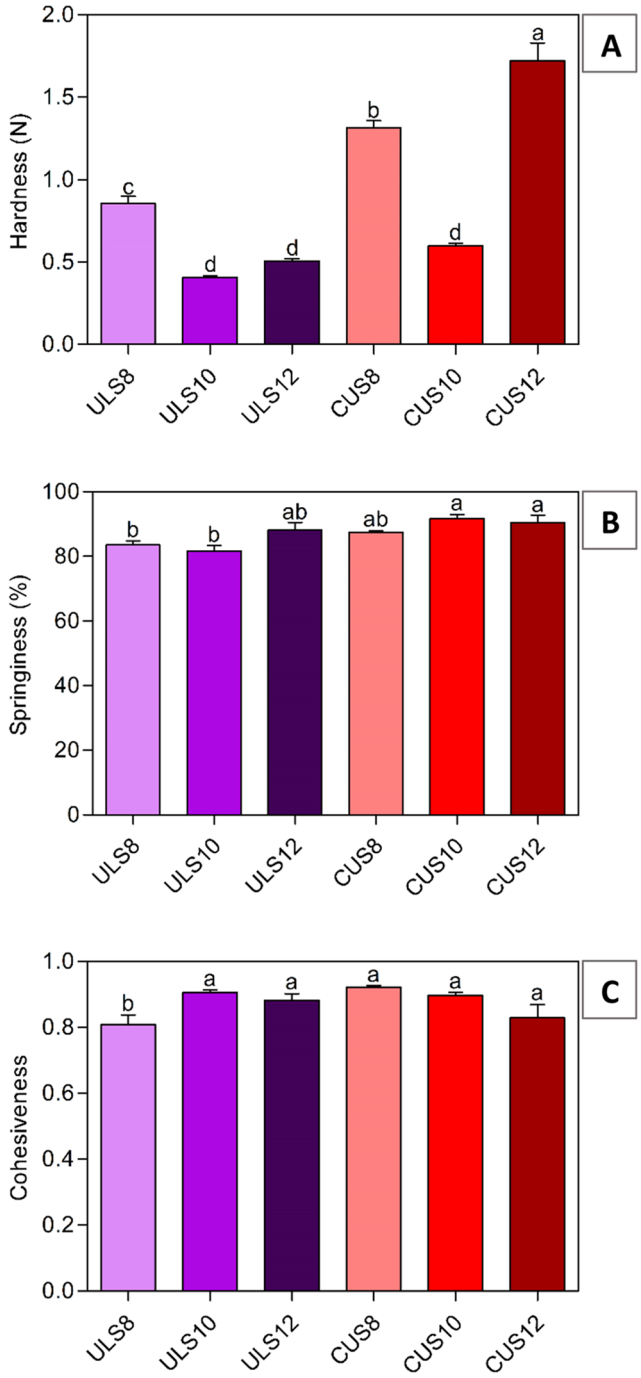


Fig. 3 Textural properties of 3D prints based on ulluco and cubio starches prepared at different starch concentrations: 8%, 10%, and 12%. Hardness (**A**), Springiness (**B**) and Cohesiveness (**C**)

and technological aspects [35]. The samples prepared with ULS had hardness values between 0.41 ± 0.02 N and 0.85 ± 0.10 N. In comparison, the samples prepared with CUS presented hardness values between 0.59 ± 0.03 N and 1.72 ± 0.24 N, with statistical differences observed between samples ($p < 0.05$).

In both cases, intermediate starch concentrations (samples ULS10 and CUS10) exhibited the lowest hardness values, which may be attributed to several factors: (i) partial or insufficient gelatinization of the material, (ii) incomplete or ineffective formation of a reticulated, lamellar, or modular microstructure, or (iii) weak interactions among the polymer chains within the matrix. On the other hand, the ULS-based samples showed the highest hardness at ULS8 (the lowest starch concentration), whereas the CUS-based samples reached their maximum hardness at CUS12 (the highest starch concentration).

The hardness results observed in the ULS samples can be explained by the microstructural analysis, which revealed the presence of irregular segments within the gel matrix of ULS10 and ULS12. This condition may hinder the structural reorganization of the gel, limiting the compaction of the material during the 3D printing process. In contrast, the ULS8 sample exhibited a more organized microstructure, suggesting that even at an 8% starch concentration, a cross-linked network can form within the gel, with pores exhibiting well-defined walls—unlike what has been reported for gels derived from other starch types [36]. This behavior may also be influenced by the starch concentration in the formulation, as a higher solid content can reduce the efficiency of network reorganization in the gel, promoting the formation of pores with incomplete or irregular walls. Furthermore, higher starch concentrations require greater energy input to achieve complete starch gelatinization [37].

In the case of the samples prepared with CUS, the higher hardness observed in CUS12 could be associated with a potentially higher degree of gelatinization achieved under the processing conditions used. This may have promoted greater leaching of amylose and amylopectin, along with improved capacity for polymer chain reorganization. As observed in the morphological analysis, this sample exhibited a highly compact microstructure, which correlates with its increased hardness. Additionally, the solid concentration in the sample may have contributed to a relative increase in amylopectin chains, favoring the formation of layered structures within the gel [36].

On the other hand, the hardness results obtained for the ULS samples can be explained by considering that the microstructural analysis revealed disorganized segments in the three-dimensional network formed in the ULS10 and ULS12 samples, whereas the ULS8 sample exhibited a more homogeneous and organized gel structure. This behavior could be related to the fact that high solid concentrations, combined with elevated gelatinization temperatures, as in the case of ulluco starch, may limit complete starch gelatinization, thereby hindering the proper formation of the three-dimensional network within the gel matrix. This structural deficiency directly results in lower compaction and,

consequently, reduced hardness in the 3D-printed material. Previous studies have shown that starch concentration is a determining factor in the degree of gelatinization, with reports indicating that in corn starches, solid concentrations equal to or greater than 10% exert an inhibitory effect on granule swelling capacity, even at temperatures as high as 90 °C [38]. It is important to note that the differences in hardness between the gels printed with CUS and ULS may be attributed to physicochemical and functional variations between the starches, but are primarily related to differences in the molecular organization of amylopectin chains within the starch granule [39]. It has been previously reported that the pasting temperature of cubio starch (CUS) is lower than that of ulluco starch (ULS), which, under the processing conditions used in this study, may have promoted a more complete gelatinization of CUS at a 12% concentration [11, 16, 20].

Previous studies have associated the hardness of starch-based 3D printed materials with the retrogradation and subsequent recrystallization of amylose and amylopectin chains [1, 40]. In addition, comparable hardness values were reported for 3D prints obtained with cassava (1.10 N), wheat (0.58 N), corn (1.21 N), sweet potato (0.64 N), potato (1.88 N), and buckwheat (1.56 N) starches [1]. The authors associated the hardness of the materials with the presence of amylopectin chains with low and high DP, finding a direct relationship between the DP of amylopectin and the hardness of the material.

The springiness attribute is related to the capacity of the 3D-printed material to recover its original shape after being subjected to a deforming force [1]. No significant differences were found between the springiness values of 3D printed samples obtained using ULS or CUS ($p>0.05$). However, differences between ULS8 and ULS10 were observed regarding the CUS10 and CUS12 samples ($p<0.05$). All samples generally had values above 0.8, indicating good material resilience, which could benefit the final product [34]. The results obtained for the analyzed samples were in agreement with values reported for 3D printing (gelatinized starch at 85 °C for 20 min) obtained from native wheat starch (0.41) and modified using a heat treatment method for 2 h (0.41) and 4 h (0.41) [35]. However, our results were higher than those obtained for 3D samples prepared with 6% potato starch, different alginate, and xanthan gum concentrations, with springiness values ranging between 0.29 and 0.65 [41].

Cohesiveness is related to the internal forces that maintain the structure of the 3D-printed material through interactions or bonds between amylose and amylopectin chains. These interactions form a three-dimensional network that resists fragmentation both during and after the printing process [3]. No statistical differences were found between the cohesiveness values of the evaluated samples ($p>0.05$), This demonstrates that the use of both starches at the established concentrations enabled the formation of structures resistant to fragmentation, even in treatments where a less homogeneous structure was observed, such as those using 10% of each starch.

The values reported in this work were similar to those obtained for 3D printing obtained from native wheat starch (0.7) and annealing wheat starch (0.8) but higher than the cohesion value of hydrothermally modified wheat starch (0.55), which the authors associated with the decreased in cohesiveness of hydrothermally modified starch due to a degradation of amylopectin chains [3].

Dynamic Mechanical Analysis of the 3D Prints

The storage (*G'*) and loss modulus (*G''*) of the analyzed samples can be observed in Fig. 4. Overall, all the samples exhibited viscoelastic behavior, with a predominant elastic character, as indicated by the higher values of *G'* compared to

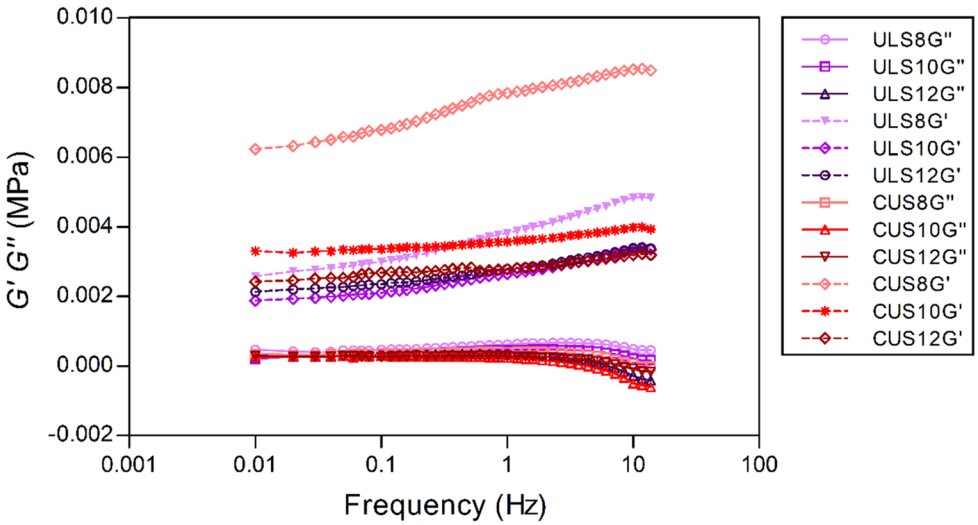


Fig. 4 Storage Modulus curves, and Loss Modulus curves of 3D prints based on ulluco and cubio starches prepared at different starch concentrations: 8%, 10%, and 12%

Table 1 Power-law parameters for frequency sweep results of 3D prints based on ulluco and Cubio starch

Sample	K (MPa Hz^{-1})	*n*'	R^2
ULS8	3713 ± 15[b]	0.151 ± 0.001[a]	0.996 ± 0.00
ULS10	2512 ± 153[c]	0.152 ± 0.001[a]	0.988 ± 0.01
ULS12	2260 ± 393[c]	0.152 ± 0.001[a]	0.993 ± 0.00
CUS8	7895 ± 247[a]	0.046 ± 0.003[b]	0.985 ± 0.00
CUS10	4159 ± 583[b]	0.151 ± 0.001[a]	0.984 ± 0.00
CUS12	2497 ± 481[c]	0.152 ± 0.001[a]	0.975 ± 0.01

Values are expressed as the mean ± SD of at least three replicates

G" throughout the analysis. Previous studies have reported similar observations regarding 3D gels produced from commercial potato puree and whole milk [42]. In this study, the authors evaluated three different formulations prepared to varying ratios of the components. They observed that the *G'* and *G"* of these materials depended on the frequency. The *G'* observed for the analyzed samples presented a direct relationship with the hardness values observed in the texture analysis, except for CU12, which showed a low *G'* value, indicating a possible syneresis process in this sample due to its high starch content. Previously, a direct relationship was reported between the values of *G'* and the hardness of 3D gels prepared with chachafruto starch and potato puree [4, 42]. This relationship was attributed to an increase in the strength of the internal structures of the 3D prints, as well as to the degree of gelatinization of the starch granules.

The parameters *K* and *n'* were obtained by fitting *G'* to the frequency sweep (Table 1). The *K* index represents the apparent viscosity of the fluid at a unit shear rate and is associated with its resistance to flow. The *n'* index indicates how this viscosity changes with shear rate: values of $n' < 1$ correspond to pseudoplastic materials, while $n' > 1$ reflect a dilatant behavior. Both parameters allow for the classification of the fluid type and the prediction of its response under stress, being essential for understanding its viscoelastic behavior in practical applications [24]. The results showed that increasing the starch concentration in both starch systems leads to a lower value of *K*, which reflects the behavior of *G'* and the strengthening of the interactions among starch chains attributed to a higher degree of gelatinization. Regarding the parameter *n'*, similar values were observed for all the samples except for CU8. This can be attributed to the fact that the frequency dependence of the materials was mainly determined by the matrix or material (starch) rather than its concentration. This finding is consistent with previous observations made for 3D printed PLA materials with cellulose nanofibers, with or without annealing treatment [25]. The authors reported that adding nanocellulose improved the elastic and viscous properties proportionally to its concentration. At the same time, the values of *n'* did not differ among the treatments, indicating that frequency dependence was not affected by the addition of nanocellulose.

Conclusions

The unconventional starches of ulluco and cubio present great 3D printability associated with the pseudoplastic fluid characteristics of the formed gels. The concentration of starch within the formulations significantly influences the characteristics of the 3D prints, primarily due to material saturation, which limits gelatinization. When examining the microstructure of 3D prints, lower starch concentrations result in less densely distributed cells but offer greater organization and better printing precision. Conversely, higher starch concentrations lead to material agglomeration in certain areas, leading to decreased printing accuracy. In terms of textural properties, all samples exhibit great resistance and resilience to deformation, significantly impacting the preservation of the physical structure of the food products produced through this technology. These samples consistently display viscoelastic behavior, with elastic properties predominating, making them comparable to 3D materials obtained by using commercial starches. Moreover, the properties observed in this study, such as printability, mechanical strength, and structural stability, highlight the potential of ulluco and cubio starches as innovative ingredients in the formulation of personalized foods, particularly for populations with specific dietary needs or preferences. Likewise, these starches could be employed in the design of 3D-printed food matrices with controlled nutrient release profiles. Their application in the development of foods with specific functional characteristics aligns with current trends in the food sector and the objectives of functional food innovation. Further research should focus on assessing the interaction of these starches with other components, particularly with those that can be included in the production of customized foods or enhancing the value of the printed products.

Acknowledgements The authors acknowledge financial support from l'Oficina de Cooperació al Desenvolupament i Solidaritat (OCDS) de la Universitat de les Illes Balears (UIB) (project OCDS-CUD2022/02) and Grant PID2019-106148RR-C43 funded by the Agencia Estatal de Investigación MCIN/AEI/ 10.13039/501100011033. We would also like to thank Dr. Joan Cifre, and Dr. Fernando Hierro Riu from the "Serveis Cientificotecnics" of the UIB for their technical assistance.

Author Contributions L.D.D.R: Conceptualization; Formal analysis; Funding acquisition; Investigation; Methodology; Writing—original draft. C.R: Formal analysis, Writing – original draft. A.S-A.: Methodology; Project administration; Resources; Supervision; Writing—original draft. H.A.V: Conceptualization; Methodology; Project administration; Resources; Supervision; Writing—original draft. V.E.: Conceptualization; Funding acquisition; Investigation; Methodology; Project administration; Resources; Supervision. All authors reviewed the manuscript.

Funding Open Access funding provided by Colombia Consortium. This work received financial support from l'Oficina de Cooperació al Desenvolupament i Solidaritat (OCDS) de la Universitat de les Illes

Balears (UIB) (project OCDS-CUD2022/02) and Grant PID2022-136889OB-C21 funded by the Agencia Estatal de Investigación MCIN/AEI/ 10.13039/501100011033.

Data Availability No datasets were generated or analysed during the current study.

Declarations

Competing Interests The authors declare no competing interests.

Open Access This article is licensed under a Creative Commons Attribution 4.0 International License, which permits use, sharing, adaptation, distribution and reproduction in any medium or format, as long as you give appropriate credit to the original author(s) and the source, provide a link to the Creative Commons licence, and indicate if changes were made. The images or other third party material in this article are included in the article's Creative Commons licence, unless indicated otherwise in a credit line to the material. If material is not included in the article's Creative Commons licence and your intended use is not permitted by statutory regulation or exceeds the permitted use, you will need to obtain permission directly from the copyright holder. To view a copy of this licence, visit http://creativecommons.org/licenses/by/4.0/.

References

1. S. Ji, T. Xu, Y. Li, H. Li, Y. Zhong, B. Lu, Food Hydrocoll. **125**, (2022)
2. N. Carvajal-Mena, G. Tabilo-Munizaga, M. Pérez-Won, C. Herrera-Lavados, R. Lemus-Mondaca, L. Moreno-Osorio, LWT. **182**, 114797 (2023)
3. L. Zheng, Q. Zhang, X. Yu, X. Luo, H. Jiang, Innov. Food Sci. Emerg. Technol. **84**, 103274 (2023)
4. L.D. Daza, M.A. Montealegre, C. Reche, A. Sandoval-Aldana, V.S. Eim, H. Alexander, Váquiro, Int. J. Biol. Macromol. **247**, 125795 (2023)
5. S.M. Kim, Y. Wen, H.W. Kim, H.J. Park, J. Food Eng. **333**, 111141 (2022)
6. A. Bebek Markovinović, P. Putnik, T. Bosiljkov, D. Kostelac, J. Frece, K. Markov, A. Žigolić, J. Kaurinović, B. Pavlić, B. Duralija, S. Zavadlav, and D. Bursać Kovačević, Antioxidants 12, (2023)
7. C. Feng, M. Zhang, 240 (2020)
8. S. Punia, S.B. Dhull, K.S. Sandhu, M. Kaur, S.S. Purewal, Legum Sci. **2**, 1 (2020)
9. S. Singh, M. Kaur, Int. J. Food Prop. **20**, 3282 (2017)
10. L. Rong, X. Chen, M. Shen, J. Yang, X. Qi, Y. Li, J. Xie, Trends Food Sci. Technol. **134**, 149 (2023)
11. A. Galindez, L.D. Daza, A. Homez-Jara, V.S. Eim, H.A. Váquiro, Carbohydr. Polym. **215**, 143 (2019)
12. H. Chen, F. Xie, L. Chen, B. Zheng, J. Food Eng. **244**, 150 (2019)
13. R. Theagarajan, J.A. Moses, C. Anandharamakrishnan, Food Bioprocess. Technol. **13**, 1048 (2020)
14. L. Zheng, Y. Yu, Z. Tong, Q. Zou, S. Han, H. Jiang, J. Food Process. Preserv. **43**, 1 (2019)
15. Y. Bugarin-Castillo, P. Rando, M. Clabaux, G. Moulin, M. Ramaioli, J. Food Eng. **350**, (2023)
16. D.O. Parra, L.D. Daza, A. Ramírez, V.S. Sandoval-Aldana, Eim, H.A. Váquiro, J. Food Process. Preserv 1 (2022)
17. B. Valcárcel-Yamani, G.G. Rondán-Sanabria, F. Finardi-Filho, Brazilian J. Pharm. Sci. **49**, 453 (2013)
18. A.C.C. Morillo, C.Y. Morillo C., and, Y.P. Tovar, L Rev. Ciencias Agrícolas. **33**, 32 (2016)
19. F.F. Velásquez-Barreto, L.A. Bello-Pérez, C. Nuñez-Santiago, H. Yee-Madeira, C.E. Velezmoro, Sánchez, Int. J. Biol. Macromol. **182**, 472 (2021)
20. L.D. Daza, M. Umaña, S. Simal, H.A. Váquiro, V.S. Eim, Int. J. Biol. Macromol. **221**, 954 (2022)
21. M.T. Pacheco, F.J. Moreno, R. Moreno, M. Villamiel, and O. Hernandez-Hernandez, Food Chem. 301, 125268 (2019)
22. M. Parra-Quijano, S. Panda, N. Rodríguez, E. Torres, Genet. Resour. Crop Evol. **59**, 49 (2012)
23. L.D. Daza, M. Umaña, S. Simal, H. Váquiro, V.S. Eim, 221, 954 (2022)
24. Z. Yang, X. Chen, Z. Xu, N. Ji, L. Xiong, Q. Sun, Int. J. Biol. Macromol. **190**, 382 (2021)
25. J. Dong, C. Mei, J. Han, S. Lee, Q. Wu, Addit. Manuf. **28**, 621 (2019)
26. Z. Liu, M. Zhang, B. Bhandari, C. Yang, J. Food Eng. **220**, 76 (2018)
27. Z. Liu, H. Chen, B. Zheng, F. Xie, L. Chen, Food Hydrocoll. **105**, 105812 (2020)
28. Y. Cheng, K. Liang, Y. Chen, W. Gao, X. Kang, T. Li, B. Cui, Food Hydrocoll. **137**, 108364 (2023)
29. D. Donmez, L. Pinho, B. Patel, P. Desam, O.H. Campanella, Curr. Opin. Food Sci. **39**, 103 (2021)
30. M. Schirmer, M. Jekle, T. Becker, Starch/Staerke. **67**, 30 (2015)
31. L.D. Daza, V.S. Eim, H.A. Váquiro, Polym. (Basel) 13, (2021)
32. S. Ahmadzadeh, A. Ubeyitogullari, Foods 11, (2022)
33. M. Esmaeelian, M. Jahani, J. Feizy, S. Einafshar, Food Biophys. **18**, 82 (2023)
34. K. Xu, M. Zhang, B. Bhandari, Food Biophys. **15**, 249 (2020)
35. B.C. Maniglia, D.C. Lima, M.M. Júnior, A. Oge, P. Le-Bail, P.E.D. Augusto, and A. Le-Bail, Food Res. Int. 137, (2020)
36. X. Xiao, L. Yang, Z. Xu, P. Huang, C. Shu, S. Song, Y. Zhang, H. Pei, Heliyon 10, e24057 (2024)
37. F. Xu, W. Liu, L. Zhang, S. Danthine, Q. Liu, F. Wang, H. Zhang, H. Hu, C. Blecker, Int. J. Food Sci. Technol. **57**, 426 (2022)
38. Z. Li, W. Liu, Z. Gu, C. Li, Y. Hong, L. Cheng, Food Hydrocoll. **48**, 189 (2015)
39. S. Wang, J. Wang, W. Zhang, C. Li, J. Yu, S. Wang, Food Chem. **181**, 43 (2015)
40. L. Zheng, J. Liu, R. Liu, Y. Xing, H. Jiang, Food Chem. **356**, 129546 (2021)
41. Y. Cui, C. Li, Y. Guo, X. Liu, F. Zhu, Z. Liu, X. Liu, F. Yang, J. Food Eng. **313**, 110756 (2022)
42. J. Martínez-Monzó, J. Cárdenas, and P. García-Segovia, Food Biophys. 14, 225 (2019)

Publisher's Note Springer Nature remains neutral with regard to jurisdictional claims in published maps and institutional affiliations.